

Physics Results and Future Plans
of
the ZEUS Experiment *

Janusz Chwastowski

Henryk Niewodniczański Institute of Nuclear Physics,
ul. Radzikowskiego 152,
31 - 342 Kraków, Poland

for The ZEUS Collaboration

3. June 2002

Abstract

Selected ZEUS results on the proton and the photon structures are presented. A short outline of the future measurements, the HERA machine and the ZEUS detector status is given.

*Presented at the 12th International Seminar on High Energy Physics, Novgorod the Great, Russia, June 1 – 7, 2002

1 Introduction

During the first decade HERA was predominantly run with 27.5 GeV leptons against 820 GeV protons. From 1998 on, the proton beam energy was increased to 920 GeV. During this time HERA reached the record value of the instantaneous luminosity $\mathcal{L} = 2 \cdot 10^{31} \text{ sec}^{-1} \text{ cm}^{-2}$. The ZEUS detector [1] collected 110 pb^{-1} of the integrated luminosity out of which about 16 pb^{-1} were taken with the electron beam.

For the neutral current (NC) reaction, $ep \rightarrow e' + X$, the four-momentum transfer can be calculated as $Q^2 = -q^2 = -(k - k')^2$ where k and k' are the incident and the scattered lepton four-momentum, respectively. The fraction x of the proton momentum carried by the struck quark is $x = Q^2/(2P \cdot q)$ with P denoting the proton four-momentum. The inelasticity is $y = (q \cdot P)/(k \cdot P)$ and $W^2 = (q + P)^2$ measures the energy of the hadronic system.

The HERA experiments extended the kinematic range by more than two orders of magnitude in both, x and Q^2 with respect to that accessible to the earlier, fixed target experiments.

2 Proton Structure

The neutral current cross section can be written in terms of the structure functions F_2 , F_L and xF_3 as

$$\frac{d\sigma^{e^{\pm}p}}{dx dQ^2} = \frac{2\pi\alpha^2}{xQ^4} [Y_+ F_2(x, Q^2) - y^2 F_L(x, Q^2) \mp Y_- x F_3(x, Q^2)]$$

where $Y_{\pm} = 1 \pm (1 - y)^2$. For Q^2 values much below the Z^0 mass the parity violating xF_3 is negligible. In LO QCD F_2 can be interpreted as a sum of the quark contributions weighted with the quark charge squared. For large Q^2 and not too small x the contribution of the longitudinal function F_L is small.

The ZEUS high precision data on F_2 are presented in Fig. 1 together with the fixed target experiments data. One can observe that F_2 slightly decreases with Q^2 for high x reflecting $q \rightarrow qg$ transitions. It becomes approximately Q^2 independent for $x \approx 0.2$ and steeply increases with Q^2 for decreasing x . This strong scaling violation reflects the influence of the $g \rightarrow qq$ splitting. These data were used in the NLO DGLAP analysis [2] to determine the parton distributions. The analysis was performed for $6.5 \cdot 10^{-5} < x < 0.65$,

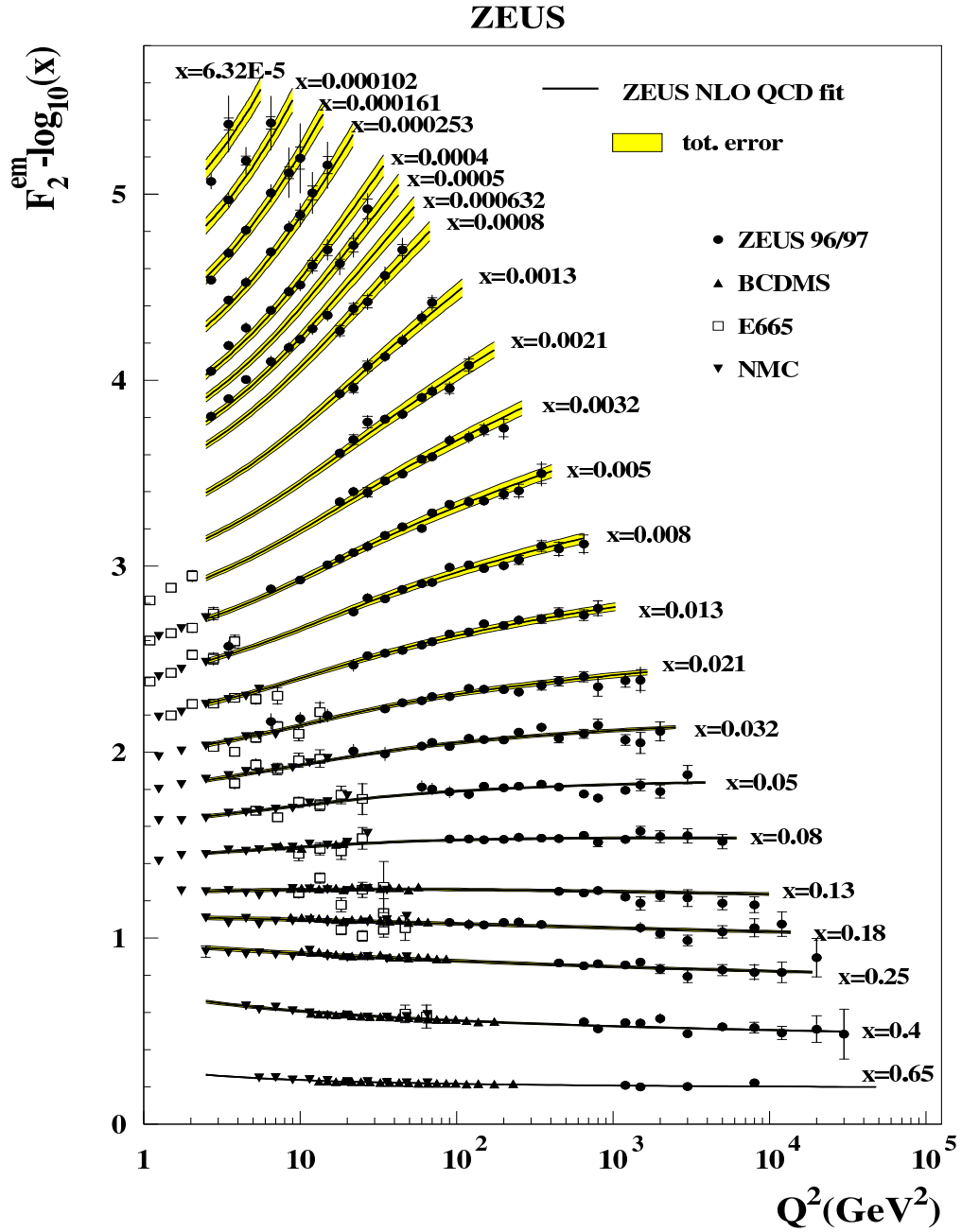


Figure 1: The ZEUS NLO QCD fit compared to the ZEUS 96/97 and fixed-target F_2 data.

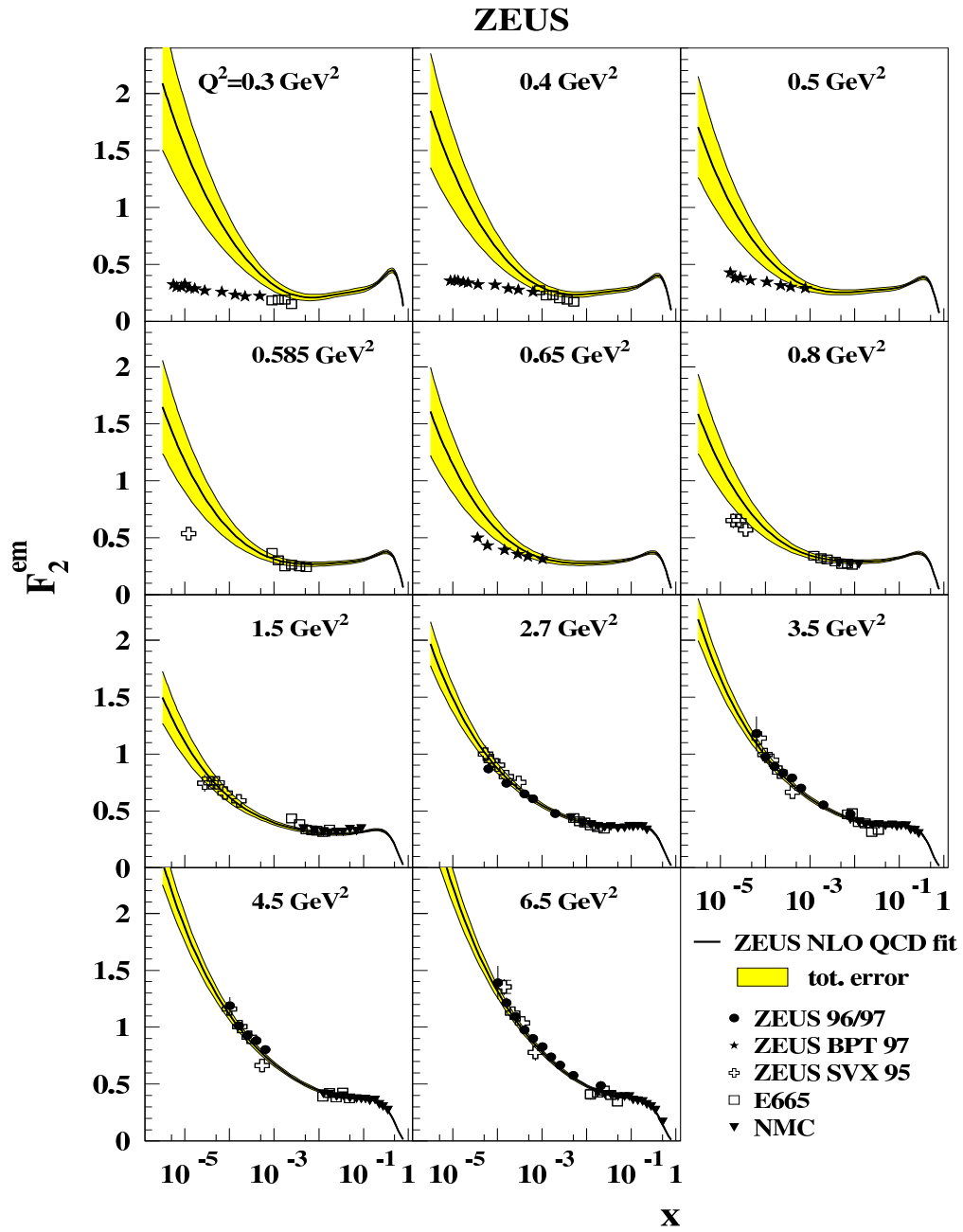


Figure 2: The ZEUS NLO QCD fit compared to the ZEUS high precision low Q^2 data.

$2.5 < Q^2 < 30000 \text{ GeV}^2$ and to diminish the higher twist contribution $W^2 > 20 \text{ GeV}$ was required. The evolution was carried out in terms of the singlet, non - singlet and gluon distributions. Fixed - target data were used to constrain the fits at high x and provide information on the valence distributions and the flavor composition of the sea.

The data are very well described by the fits. It was checked that the ZEUS NLO parametrisations of the parton distributions are in good agreement with other [3, 4] parametrisations. The gluon distribution was found to be valence like at small Q^2 and for increasing Q^2 it shows very strong increase with decreasing x . The sea distribution is flat at small Q^2 and it increases with decreasing x for higher values of Q^2 . However, this increase is much weaker than the one seen in case of the gluon distribution. The longitudinal structure function F_L is valence like for relatively small Q^2 . At $Q^2 \approx 1 \text{ GeV}^2$ it appears to be negative however compatible with zero within the errors. The fit results were compared to high precision low Q^2 data [5]. This comparison is shown in Fig. 2. The data are well reproduced for $Q^2 \gtrsim 1.5 \text{ GeV}^2$. Below, the discrepancies between the data and the fit results are large. Also, F_L shows a non-physical behaviour for small Q^2 . This clearly shows limitations of the DGLAP fit application.

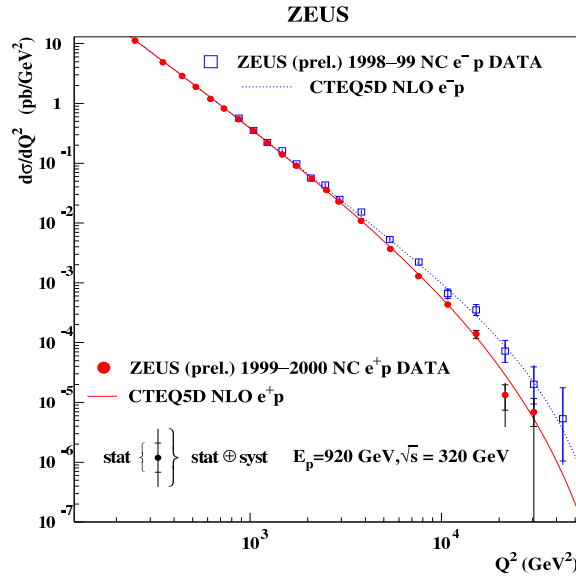


Figure 3: The differential $e^\pm p$ NC cross sections compared to the SM expectations evaluated using CTEQ5D PDF.

The neutral current cross section was measured for $Q^2 > 185 \text{ GeV}^2$ [6]. The data are presented in Fig. 3 together with the Standard Model (SM) predictions. A clear dominance of the photon exchange is seen for $Q^2 \leq 3000 \text{ GeV}^2$. Above this value the $\gamma - Z^0$ interference becomes visible. The data are well described by the the parametrisations and the ZEUS NLO fit results. However, particularly, for high Q^2 they are statistically limited. The $x F_3$ structure function was extracted for $Q^2 > 3000 \text{ GeV}^2$ and was found to be well described by the SM motivated parametrisations.

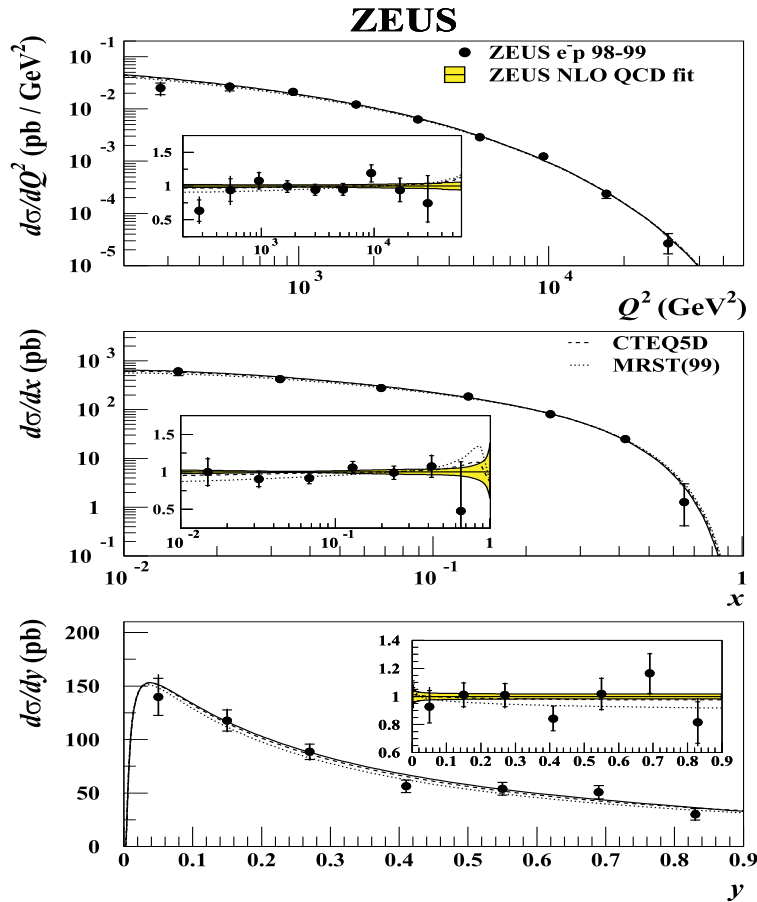


Figure 4: The e^-p CC cross sections compared to the ZEUS NLO QCD fit, CTEQ5D and MRST(99) PDFs. The insets show the ratios of the measured cross sections to the SM expectations evaluated using ZEUS NLO QCD fit.

The cross section for the charged current (CC) reaction, $ep \rightarrow \nu + X$,

was measured for $Q^2 > 200 \text{ GeV}^2$ [7]. The data together with the ZEUS NLO and other parametrisations are shown in Fig. 4. The data are very well described by the parametrisations over several orders of magnitude. They were used to extract value of the mass of the W boson – M_W . The fit was performed to the shape of the cross section. In the fit the Fermi constant was fixed to its *PDG* value $G_F = 1.11639 \cdot 10^{-5} \text{ GeV}^{-2}$ [8]. The fit yielded $M_W = 80.3 \pm 2.1(\text{stat.}) \pm 1.2(\text{syst.}) \pm 1.0(\text{pdf}) \text{ GeV}$ for the electron data. This value well compares to the positron data result of: $M_W = 81.4_{-2.6}^{+2.7}(\text{stat.}) \pm 2.0(\text{syst.})_{-3.0}^{+3.3}(\text{pdf}) \text{ GeV}$ [9], the *PDG* value: $M_W = 80.422 \pm 0.047 \text{ GeV}$ and to the H1 result [10].

3 Photon Structure

In photoproduction at HERA a quasi – real photon emitted by the electron interacts with a proton. The LO QCD divides such interactions into two classes. In resolved processes a photon acts as source of partons and only a fraction of its momentum, x_γ , participates in hard scattering. In direct processes the photon interacts via the boson – gluon fusion or the QCD Compton and acts as a point-like particle with $x_\gamma \approx 1$. The measurements of the jet cross section in photoproduction [11, 12] are sensitive to the proton and photon structures, and to the dynamics of the hard sub-process.

Since x_γ is not measured directly then x_γ^{obs} - the fraction of the photon momentum participating in the production of the two highest energy jets was introduced [13]

$$x_\gamma^{obs} = \frac{E_T^{jet1} e^{-\eta_{jet1}} + E_T^{jet2} e^{-\eta_{jet2}}}{2 y E_e}$$

where $E_T^{jet1,2}$ are the transverse energies of the jets in the LAB frame, $\eta_{jet1,2}$ are the jets pseudorapidities and y is the fraction of the lepton energy, E_e , carried by photon in the proton rest frame. In the LO QCD $x_\gamma^{obs} = x_\gamma$. It was shown [11] that the resolved component dominated region for $x_\gamma^{obs} < 0.75$. Above this value the direct component dominates.

The distribution of angle, Θ^* , between the jets in the parton – parton CMS is sensitive to the form of the matrix element. For direct processes, mediated by the quark, the distribution $d\sigma/d\cos\Theta^* \sim (1 - \cos\Theta^*)^{-2}$. If the process is mediated by the gluon exchange, like in case of the resolved component, then $d\sigma/d\cos\Theta^* \sim (1 - \cos\Theta^*)^{-1}$. Fig. 5 shows the angular distributions

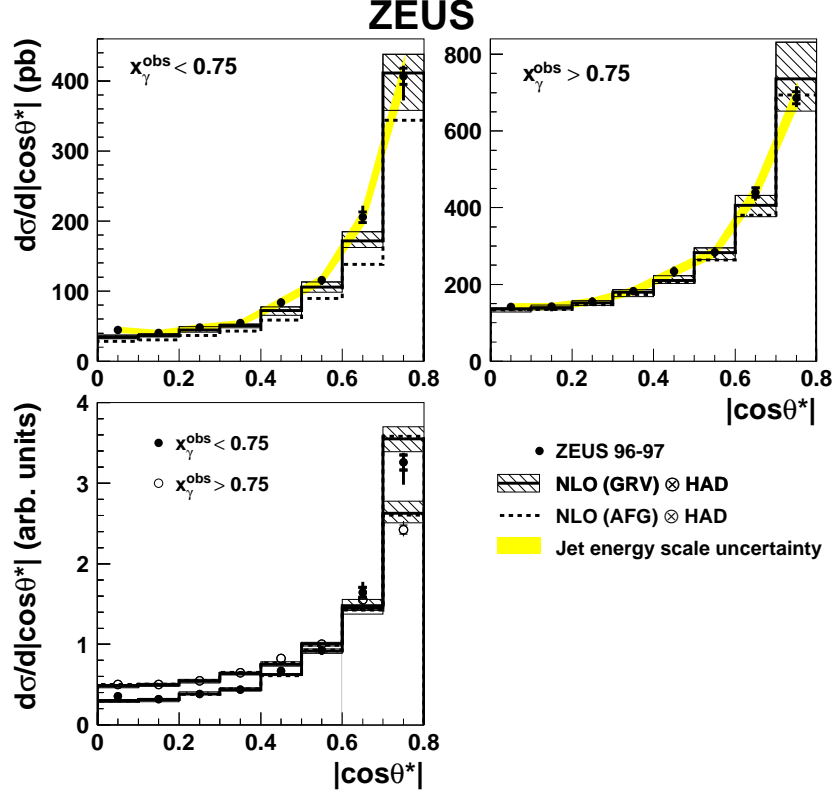


Figure 5: The $|\cos\theta^*|$ distribution for jets for the resolved ($x_\gamma^{obs} < 0.75$) and direct ($x_\gamma^{obs} > 0.75$) component dominated regions, and comparison of the shapes of the $|\cos\theta^*|$ distributions (left bottom).

in the resolved and direct component dominated regions together with the NLO QCD predictions of [14] which include different parametrisations of the photon PDFs: GRV-HO [15] and APG-HO [16]. The CTEQ5M1 [17] proton PDF was used in the calculations and the hadronisation corrections were estimated with HERWIG [18] and PYTHIA [19] Monte Carlos.

For $x_\gamma^{obs} < 0.75$ the data are underestimated by the calculations' results by about 10-20%. The GRV-HO delivers better description of the data. For $x_\gamma^{obs} > 0.75$ the data are well reproduced by the calculations. The shapes of the angular distributions for both regions are compared in Fig. 5 (left bottom). Also the results of the NLO calculations are shown. In general the data are well reproduced by the calculations. The distribution measured

for $x_\gamma^{obs} < 0.75$ is steeper than the one for $x_\gamma^{obs} > 0.75$. This confirms the differences in the dominant propagators.

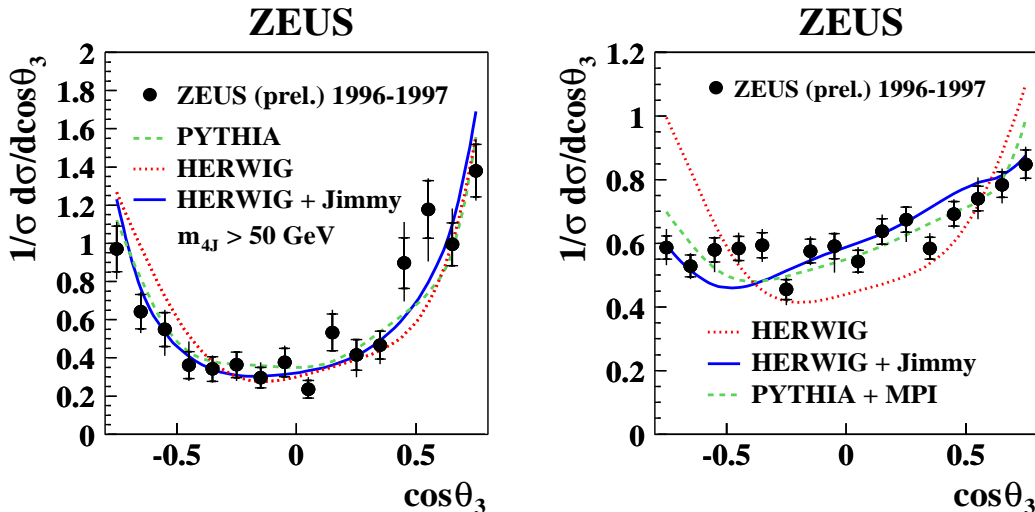


Figure 6: The $\cos\theta_3$ distribution for the high jets mass region ($M_{4j} > 50$ GeV) (left) and for “inclusive” sample (right).

The photon structure can also be looked at in multi-jet events. The four jet production is sensitive to QCD at α_s^3 and to the multi-parton interactions in the final state. Since it is difficult to manipulate four objects then the number of jets is reduced. Namely, two jets with the lowest invariant mass are combined into one. Afterward, the jets are re-ordered in energy. The dynamics is investigated looking at the distribution of $\cos\Theta_3$, the angle between the proton and the most energetic jet directions. This distribution is shown in Fig. 6 together with the MC models’ predictions. In the “perturbative” region, for the four-jet mass $M_{4j} > 50$ GeV, the distribution is peaked in the forward and backward directions. The data are well described by the shown MC irrespectively whether or not the multi-parton interaction (MPI) option is included into the calculations. In case of the “inclusive” sample the distribution increases with increasing $\cos\Theta_3$. The data are well described by the MC models with the MPI option included. The HERWIG without the MPI fails to reproduce the data.

The total cross section for the photoproduction was recently re-measured [20]. The data used came from dedicated runs. This allowed the control

and reduction of the systematic errors. The total cross section measured at $W = 209$ GeV was found to be

$$\sigma_{TOT}^{\gamma p} = 174 \pm 1(stat.) \pm 13(syst.)\mu b.$$

The result is compatible with the H1 result [21] and the value predicted by the Donnachie and Landshoff [22].

4 Future Plans

The increase of the luminosity and the longitudinal polarisation for ZEUS and H1 are the main goals of the HERA upgrade programme. These goals are achieved by the introduction of the mini beta focusing scheme (about 3.5 times increase in luminosity) and the spin rotators. It is expected to collect 1000 pb^{-1} during few years of running. The luminosity will be shared equally between the different lepton beam charges and polarisations. Runs with decreased proton beam energy for the F_L and high x measurements are foreseen. Presently, the main stress is put on the background reduction in the experimental areas and the beams' currents increase.

The physics programme was discussed in great detail in [23]. Below only few examples are given. In general the precision tests require 3-10 times increase in the luminosity. Longitudinal polarisation of the lepton beam will help to pin down some problems.

As an example, the influence of the degree of polarisation, P , on the light quark coupling determination [24] is presented in Fig. 7. The anticipated size of the error on the u quark coupling decreases significantly with increasing degree of the lepton beam polarisation. Possible new physics can demonstrate itself by a deviation from the linear dependence of the charged current cross section on the polarisation. Hera is also a potential source of its "own" particle density functions. The PDFs measurement within a single experiment over whole phase space offers a unique possibility of the understanding, control and uniform treatment of systematic effects. Such measurements require improved measurement and reconstruction of the kinematics especially at high x and Q^2 . Since the tracks in such events are collimated in the forward (proton) direction the detector performance in this region has to be improved. Improvements of the vertexing and tracking will play important role in the heavy quark studies after the upgrade. Presently, the measurement of the $F_2^{c\bar{c}}$ [25] suffers from the statistical limitations of the data sample.

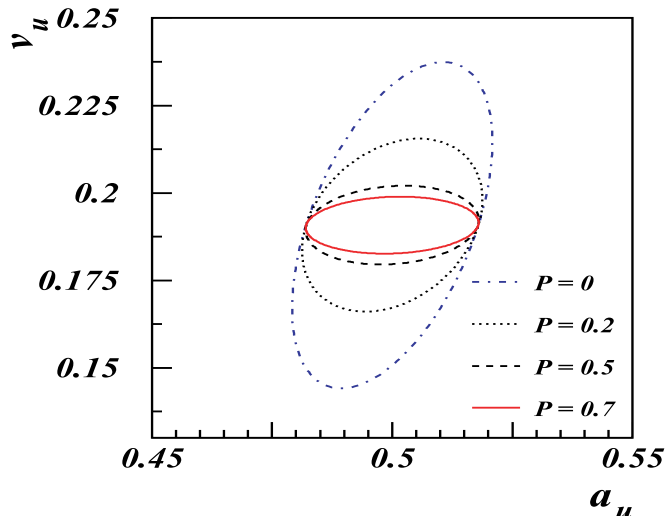


Figure 7: Sensitivity of the errors on the u quark coupling to beam polarisation, P (from [24]).

It is clear that the precise tracking and secondary vertex finding will improve the measurement. It will also help to resolve the problem of the discrepancy between the data and the NLO calculations of the b quark production.

The ZEUS detector upgrade followed the physics programme. A new silicon micro-vertex detector (MVD) [26] and the forward, straw-tube tracker (STT) [27] were installed. The MVD covers range of 10 – 160 degrees of the polar angle. It consists of three forward wheels and the barrel part centered on the interaction point. This detector will be used for the precise tracking and the reconstruction of displaced vertices. The device will be used for the study of the heavy flavor production and will improve the charged current physics. The second device, the STT, has four layers of the highly efficient, straw tube drift chambers. It extends the tracking range by more than a unit in pseudorapidity and covers the range of 5 – 25 degrees of the polar angle. Good tracking and vertexing abilities will help in the electroweak and exotics studies with high x and Q^2 events. It will be complementary to the MVD for the heavy flavor studies. Also the vector meson and the QCD studies will profit from the extension of the W range.

Presently the ZEUS detector is tested and waiting for the data taking period.

5 Acknowledgements

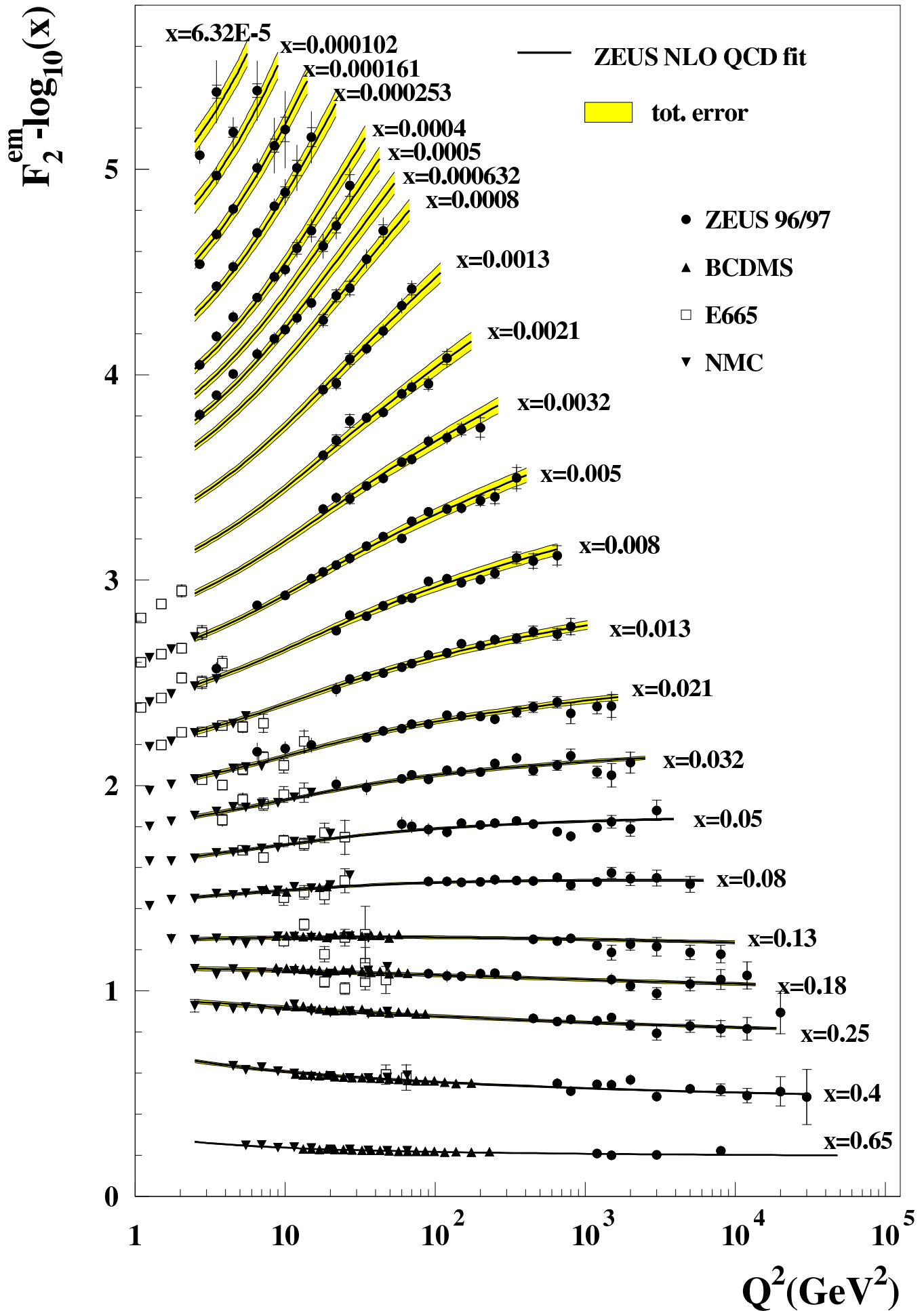
I thank the organisers for the invitation and for the stimulating and enjoyable atmosphere they provided. I am grateful to M. Derrick, M. Kuze and E. Tassi for discussions. The DESY Directorate financial support is kindly acknowledged.

References

- [1] The ZEUS Detector Status Report (unpubl.), U. Holm(ed), DESY, 1993.
- [2] ZEUS Coll., S. Chekanov et al., DESY-02-105.
- [3] J. Pumplin et al., Preprint hep-ph/0201195, 2002.
- [4] A. D. Martin et al., Preprint hep-ph/0110215, 2002.
- [5] ZEUS Coll., J. Breitweg et al., Eur. Phys. J. **C 7**, 609 (1999),
ZEUS Coll., J. Breitweg et al., Phys. Lett. **B 487**, 53 (2000).
- [6] ZEUS Coll., S. Chekanov et al., DESY-02-113,
ZEUS Coll., presented by M. Moritz at DIS 2002, Cracow.
- [7] ZEUS Coll., S. Chekanov et al., Phys. Lett. **B 539**, 197 (2002).
- [8] Particle Data Group, D. E. Groom et al., Eur. Phys. J. **C 15** 1 (2000).
- [9] ZEUS Coll., J. Breitweg et al., Eur. Phys. J. **C 12**, 411 (200).
- [10] H1 Collab., C. Adloff et al., Eur. Phys. J. **C 13**, 609 (2000).
- [11] ZEUS Coll., S. Chekanov et al., Eur. Phys. J **C 23**, 13 (2002).
- [12] H1 Collab., C. Adloff et al., DESY-01-225 and hep-ex/0201006.
- [13] ZEUS Coll., M. Derrick et al., Phys. Lett. **B 348**, 665 (1995).
- [14] S. Frixione, Z. Kunszt and A. Signer, Nucl. Phys. **B 467**, 399 (1996),
S. Frixione, Nucl. Phys. **B 507**, 295 (1997),
S. Frixione and G. Ridolfi, Nucl. Phys. **B 507**, 315 (1997).

- [15] M. Glück, E. Reya and A. Vogt, Phys. Rev. **D 45**, 3986 (1992), Phys. Rev. **D 46**, 1973 (1992).
- [16] P. Aurenche, J. Guillet and M. Fontannaz, Z. Phys. **C 64**, 621 (1994).
- [17] H. L. Lai et al., Phys. Rev. **D 55**, 1280 (1997).
- [18] G. Marchesini et al., Comp. Phys. Comm., **67**, 465 (1992).
- [19] T. Sjöstrand, Comp. Phys. Comm., **82**, 74 (1994).
- [20] ZEUS Coll., S. Chekanov et al., Nucl. Phys. **B 627**, 3 (2002).
- [21] H1 Coll., S. Aid et al., Phys. Lett. **B 299**, 374 (1993), Z. Phys. **C 69**, 27 (1995).
- [22] A. Donnachie and P. V. Landshoff, Phys. Lett. **B 437**, 408 (1998).
- [23] Future Physics at HERA, Proc. of the Workshop 1995/96, eds. G. Ingelmann, A. De Roeck, R. Klanner.
- [24] R. J. Cashmore et al., in Future Physics at HERA, Proc. of the Workshop 1995/96, eds. G. Ingelmann, A. De Roeck, R. Klanner, p. 163.
- [25] ZEUS Coll., J. Breitweg et al., Eur. Phys. J. **C 12**, 35 (2000).
- [26] E. Koffeman, NIM **A 473**, 26 (2001).
- [27] ZEUS Coll., A Straw-Tube Tacker for ZEUS, Jun. 1998 (unpubl.).

ZEUS



ZEUS

